BBA - General Subjects 1864 (2020) 129656

Contents lists available at ScienceDirect

BBA - General Subjects

journal homepage: www.elsevier.com/locate/bbagen

Rab7 of *Plasmodium falciparum* is involved in its retromer complex assembly near the digestive vacuole

Asim Azhar Siddiqui, Debanjan Saha, Mohd Shameel Iqbal, Shubhra Jyoti Saha, Souvik Sarkar, Chinmoy Banerjee, Shiladitya Nag, Somnath Mazumder, Rudranil De, Saikat Pramanik, Subhashis Debsharma, Uday Bandyopadhyay*

Division of Infectious Diseases and Immunology, CSIR-Indian Institute of Chemical Biology, 4, Raja S. C. Mullick Road, Jadavpur, Kolkata 700032, West Bengal, India

ARTICLE INFO

Keywords:
Plasmodium falciparum
Rab7
GTPase
Digestive vacuole
Retromer complex

ABSTRACT

Background:

Intracellular protein trafficking is crucial for survival of cell and proper functioning of the organelles; however, these pathways are not well studied in the malaria parasite. Its unique cellular architecture and organellar composition raise an interesting question to investigate.

Methods:

The interaction of *Plasmodium falciparum* Rab7 (*Pf*Rab7) with vacuolar protein sorting-associated protein 26 (*Pf*VPS26) of retromer complex was shown by coimmunoprecipitation (co-IP). Confocal microscopy was used to show the localization of the complex in the parasite with respect to different organelles. Further chemical tools were employed to explore the role of digestive vacuole (DV) in retromer trafficking in parasite and GTPase activity of *Pf*Rab7 was examined.

Results:

*Pf*Rab7 was found to be interacting with retromer complex that assembled mostly near DV and the Golgi in trophozoites. Chemical disruption of DV by chloroquine (CQ) led to its disassembly that was further validated by using compound 5f, a heme polymerization inhibitor in the DV. *Pf*Rab7 exhibited Mg^{2+} dependent weak GTPase activity that was inhibited by a specific Rab7 GTPase inhibitor, CID 1067700, which prevented the assembly of retromer complex in *P. falciparum* and inhibited its growth suggesting the role of GTPase activity of *Pf*Rab7 in retromer assembly.

Conclusion:

Retromer complex was found to be interacting with *Pf*Rab7 and the functional integrity of the DV was found to be important for retromer assembly in *P. falciparum*.

General significance:

This study explores the retromer trafficking in *P. falciparum* and describes amechanism to validate DV targeting antiplasmodial molecules.

1. Introduction

Plasmodium falciparum is an intracellular parasite that infects the erythrocytes of its host. The intraerythrocytic stages of the parasite are responsible for its pathogenesis when it digests host hemoglobin in its DV that is a temporary organelle formed only during intraerythrocytic stages of the parasite [1]. DV is often regarded as the metabolic headquarter of the parasite and a known target for several antiplasmodial compounds [2]. The parasite thrives in the host erythrocyte and depends on its hemoglobin for nutrition and growth. It has a specialized machinery of various proteases to digest host hemoglobin inside DV [3]. Hemoglobin digestion in DV results in the release of free heme that is highly toxic to the cell. The DV of the parasite utilizes a unique mechanism where it converts free heme into an insoluble and non-toxic crystalline pigment called hemozoin [4]. Because of these factors, DV is one of the most potential targets of antiplasmodial molecules. Organellar architecture of *Plasmodium* is highly dissimilar from other eukaryotes. It has a very unusual single mitochondrion per cell [5], its endoplasmic reticulum is not well defined [6], Golgi bodies in *Plasmodium* are primitive [7]. This peculiar organization of organelles

* Corresponding author.
E-mail address: udayb@iicb.res.in (U. Bandyopadhyay).

https://doi.org/10.1016/j.bbagen.2020.129656
Received 24 January 2020; Received in revised form 22 April 2020; Accepted 2 June 2020
Available online 05 June 2020

indicates towards a complex and atypical protein trafficking machinery in the parasite through which it needs to precisely transport its proteins. DV has an acidic pH and a battery of proteolytic enzymes that make it functionally similar to the lysosome [2,8]. It is considered equivalent to an endolysosomal compartment in parasite because of some similar features, however, this comparison is still inaccurate because of some basic dissimilarities in them, for example, their contents, biogenesis and protein targeting [9]. Endocytosis has been reported in *Plasmodium* for the uptake of host hemoglobin through cytostomes where hemoglobin digestion starts and these vesicles subsequently fuse with the DV [10,11]. Little is known about protein trafficking from the Golgi to these organelles [12]. In the intra-erythrocytic stages of *Plasmodium*, endocytosis of host hemoglobin occurs by several different mechanisms that led to the formation of its DV [13]. The crosstalk between *de novo* generated DV and its single compartment Golgi body presents an important problem that is required to be investigated.

A number of proteins are required to maintain the functioning of organelles in cells. Among them, Rab GTPases act as master regulators for the functioning of such membrane bound organelles [14]. Rab proteins belong to the Ras superfamily of proteins which are small GTPases involved in a varied range of cellular functions [15]. Their important role in phagosome maturation makes them a crucial factor in intracellular parasite and host interactions [16]. Rab GTPases have two conformations: GTP-bound (active) and GDP-bound (inactive) [17]. Interchange between these two conformations induces various structural changes in the proteins [18]. Moreover, Rab proteins need to get prenylated to perform their function at C-terminal cysteine motifs which attach them to the membranes [19]. Different Rab proteins are localized in different cellular compartments depending on their functions, for example, early endosomes are marked by Rab5 and late endosomes by Rab7 [20]. *Plasmodium* too, like other eukaryotes, deploys many Rab proteins for such pathways indicating that Rab proteins regulated vesicular transportation and endosomal system in the parasite [21]. Rab7, in mammalian cells, is required for the recruitment of retromer complex [22]. It is a late endosomal marker and a regulator of retromer complex as previously shown in yeast and human cells [23,24]. Co-IP studies have established the interaction between Rab7 and retromer complex [23,25] and a previous report has described Rab7 in *P. falciparum* [26]. Retromer complex is a coat protein complex required for the retrieval of sorting receptors from late endosome to trans-Golgi network [27]. It consists of a core trimer of VPS35, VPS29 and VPS26 that may be associated with a variety of regulatory proteins and members of SNX protein family like SNX1/SNX2 and SNX5/SNX6 in yeast [28–30].

In this study, we cloned and purified *Pf*Rab7 and explored its interaction with retromer complex in *P. falciparum* with respect to DV of the parasite using different chemical tools. *Pf*Rab7 was found to be closely associated with Golgi and DV of the parasite in most of the trophozoites indicating an obscure endosomal like system in *P. falciparum*. *Pf*Rab7 was found to be interacting with retromer complex and the retromer assembly was found to be affected by selective disruption of DV by CQ. This was further endorsed by using a hemozoin inhibitor, compound 5f, in *P. falciparum* CQ sensitive 3D7 strain and CQ resistant K1 strain. *Pf*Rab7 was found to be interacting with retromer complex in *P. falciparum* as shown by co-IP experiments. We evaluated the intrinsic enzymatic GTPase activity of the recombinant *Pf*Rab7 and its inhibition by CID 1067700 which was later found to be antiparasitic. The study provides insight into the retrograde pathway in *Plasmodium* with the involvement of DV and role of Rab7 which can be crucial in designing novel strategiesfor antimalarial drug development.

2. Material and methods

2.1. Bioinformatics analysis of PfRab7

*Pf*Rab7 sequence was retrieved from PlasmoDB (Gene ID PF3D7_0903200). BLASTp programme was used for homology search. Multiple sequence alignment of *Pf*Rab7 and Rab7 from other organisms (*Pv - Plasmodium vivax, Pk - Plasmodium knowlesi, Pc - Plasmodium chabaudi, Py - Plasmodium yoelii, Pb - Plasmodium berghei, Cp - Cryptosporidium parvum, Mm - Mus musculus, Hs - Homo sapiens* and *Sc - Saccharomyces cerevisiae*) was performed by the MAFFT software and visualized by Jalview program. 3D structure of *Pf*Rab7 was predicted by an online server I-TASSER [31,32]. Subsequent analysis was done by using BIOVIA Discovery Studio Visualizer and PyMOL softwares. For *in silico* interactome analysis of *Pf*Rab7 and *Pf*VPS26, online STRING database (https://string-db.org/) was used.

2.2. Parasite culture and calculation of IC_{50}

P. falciparum (3D7 and K1 strains) were cultivated by the method as previously described [33,34]. In brief, parasites were cultured *in vitro* in complete RPMI medium containing RPMI 1640 medium supplemented with 25 mM HEPES (Sigma-Aldrich), 1.96 g/l D-(+)-glucose (Sigma-Aldrich), 1.76 g/l sodium bicarbonate (Sigma-Aldrich), 50 μg/ml gentamycin (Amresco), 370 μM hypoxanthine (Sigma-Aldrich) and 0.5% (*w/v*) AlbuMaxII (Thermo Fisher Scientific) with a final pH 7.2 and at a hematocrit level of 5% in tissue-culture flasks kept inside candle jars placed in CO_2 cell culture incubator at 37 °*C*.Medium change was given every 24 h and the culture was monitored through Giemsa staining of thin smears of RBCs.

The IC_{50} of CID 1067700 (Sigma-Aldrich) was calculated by SYBR Green assay as previously described [35]. In brief, parasite culture with 1% parasitemia and 2% hematocrit was incubated at 15 different concentrations (serial 1:2 dilution starting from 40 μM) of CID 1067700 for 48 h in 96 well plate with 100 μl culture in each well. After treatment, parasite cells in each well were lysed in 100 μl of 20 mM Tris buffer with pH 7.5 containing 5 mM EDTA, 0.008% (weight/volume) saponin, 0.008% (volume/volume) Triton X-100 and 2× SYBR green I stain [36,37]. After 1-h incubation, the fluorescence from plate was measured at 485 nm excitation and 530 emission in a fluorimeter. This assay measures the growth of parasite. The concentrations of compound were plotted against the percent fluorescence intensity measured by using DMSO as control in culture (at 0 concentration of compound). IC_{50} was calculated by quantitative analysis of data with non-linear regression by GraphPad Prism 6 software.

2.3. Compounds treatment

For confocal microscopy experiments, 2 ml synchronized parasite culture containing young trophozoites with 5% parasitemia was incubated in presence of different compounds as follows: CID 1067700 (10 μM) for 2 h, CQ (20 nM) for 4 h, Compound 5f (15 μM) for 4 h and atovaquone (20 nM) for 4 h. For light microscopy, parasite was treated with CID 1067700 (10 μM) for 8 h and slides were prepared after methanol fixation using Giemsa staining. Cells were then used for microscopic studies.

2.4. Parasite synchronization and lysate preparation

Parasite culture was synchronized by using 5% sorbitol solution. In brief, the medium was removed from the culture and cells were washed by sterile PBS (Phosphate buffered saline, 137 mM sodium chloride, 2.7 mM potassium chloride, 10 mM disodium hydrogen phosphate and 1.8 mM potassium dihydrogen phosphate), followed by incubation in sterile 5% D-sorbitol solution in distilled water for 20 min at 37 °C in cell culture incubator. Cells were then washed thrice with RPMI 1640 media and placed back in a fresh culture flask with complete RPMI. The procedure was repeated after 4 h for tight synchronization.

For parasite isolation, infected RBCs were centrifuged at 800 ×*g* for 4 min in a tube, washed, and resuspended in cold PBS (Amresco). Next, an equal volume of 0.2% saponin in PBS (final concentration 0.1%) was

added and cells were kept on ice for 15 min. The tube was then centrifuged at 1500 ×*g* for 8 min to collect the parasites, which were washed with PBS and either used immediately or stored at −80 °C for future use. To prepare parasite lysate, cells were suspended in co-IP buffer (10 mM HEPES, 50 mM NaCl, 0.004% Nonidet P-40, pH 7.4) and lysed by sonication (10 s pulse and 30 s rest cycle alternately at an amplitude of 20%) for 120 s (total 30 s of sonication and 90 s of rest) in a sonicator.

2.5. PfRab7 purification and MALDI MS/MS

Chemically synthesized *Pf*Rab7 gene (PlasmoDB ID: PF3D7_1250300) cloned in pET28a (+) DNA vector (Novagen) was procured from GenScript. For protein expression, *Pf*Rab7 containing pET28a plasmid was transformed in *E. coli* Rosetta competent cells (Novagen). Five milliliter of LB (Luria Bertani) broth (Himedia) with 50 μg/ml kanamycin and 40 μg/ml chloramphenicol was inoculated with a single colony picked from transformed Rosetta cells and allowed to grow overnight at 37 °C with shaking at 200 rpm. 1% (*v*/v) of this culture was used to inoculate 1000 ml LB broth containing same antibiotics and kept in shaker-incubator with constant shaking at 200 rpm set at 37 °C. The culture was induced by IPTG (Thermo Fisher Scientific) at the concentration of 1 mM when its OD_{600} reached 0.5–0.6 and kept for 5 h in a 37 °C shaker for protein expression. Next, cells were collected by centrifugation at 6000 ×*g* for 5 min at 4 °C, then suspended in 20 ml of lysis buffer (50 mM Tris HCl, pH 8.0, 300 mM NaCl, 10 mM imidazole and 10% glycerol) with lysozyme (1 mg/ml) and protease inhibitor cocktail (Calbiochem). Cells were kept at 4 °C for 2 h followed by lysis using sonication (12 s pulse and 30 s rest cycle at an amplitude of 70%) for 40 min (total 11.4 min of sonication and 28.6 min of rest). The lysate was cleared by ultra-centrifugation at 40,000 ×*g* for 40 min at 4 °C. The supernatant was incubated with Ni-NTA agarose resin (Qiagen) equilibrated with lysis buffer for 2 h under agitation at 4 °C. Ni-NTA agarose beads were allowed to settle and the lysate was allowed to flow out from the column. This was followed by washing of resin poured in a column with 500 ml of cold wash buffer (50 mM Tris HCl, pH 8.0, 300 mM NaCl, 60 mM imidazole and 10% glycerol) at 4 °C. Recombinant *Pf*Rab7 was eluted in 10 fractions of 1.5 ml each by cold elution buffer (50 mM Tris HCl, pH 7.5, 300 mM NaCl, 250 mM imidazole and 10% glycerol) and checked on 12% SDS-PAGE for purity. Pure fractions were collected and dialyzed to remove imidazole and estimated by Bradford protein assay. Eluted protein was checked on SDS-PAGE followed by staining with Coomassie Brilliant Blue R-250 and the band was sliced out for tryptic digestion by In-Gel Tryptic Digestion kit (Thermo Fisher Scientific) using the method previously described [38]. In short, gel band with protein was de-stained in ammonium bicarbonate and acetonitrile solution followed by reduction with Tris (2-carboxyethyl) phosphine (TCEP) and alkylation by Iodoacetamide. Then the gel was shrunk by acetonitrile, then activated trypsin was added for overnight at 30 °C and the peptides were extracted after adding trifluoroacetic acid to inactivate the trypsin. It was followed by MALDI MS/MS where small peptides from digested protein were identified to predict the protein with a score by proteomics service Matrix Science (version 2.1), where mass spectral data were submitted to Mascot Database search program.

2.6. GTPase assay

GTPase assay was performed with recombinant *Pf*Rab7 to analyze its enzymatic activity. Twenty microgram of protein was incubated with eight different concentrations of GTP starting from 5 mM that was diluted serially by 1:2 to calculate the K_m, V_{max} and k_{cat} in 20 mM Tris buffer pH 7.5, 100 mM NaCl and 1 mM $MgCl_2$ at 37 °C for 2 h in a total volume of 50 μl at 37 °C and atmospheric pressure. K_m, V_{max} and k_{cat} were determined by nonlinear regression analysis using GraphPad Prism version 6.0 software. Released phosphate was estimated by Malachite green assay using BIOMOL Green (Enzo) as described in the user manual. To check the effect of inhibitors, 10 μg of recombinant *Pf*Rab7 was incubated for 4 h at 37 °C with different concentrations (0, 50, 100, 150, 200 μM) of inhibitors (CID 1067700, Sigma-Aldrich and Dynasore hydrate, Sigma-Aldrich) and EDTA (as mentioned in figures) along with 50 μM GTP. Released phosphate was estimated as Malachite green assay using BIOMOL Green (Enzo).

2.7. PfVPS26 cloning

For cloning of *Pf*VPS26 (PlasmoDB ID: PF3D7_0903200), *E. coli* expression vector pET11a was used for the overexpression of protein. For gene cloning, the cDNA obtained was PCR amplified with forward primer 5′- CTCTCTCATATGCTATCTACAATTTTTGGGAGCG −3′ (Nde I restriction site was underlined) and reverse primer 5′- TTCAGGATCC CTAACCCATTTTTTTTCGCCATAAG −3′ (BamH I restriction site was underlined) in a total volume of 50 μl using DreamTaq DNA Polymerase (Thermo Fisher Scientific) with conditions: initial denaturation at 95 °C for 3 min followed by 35 cycles of 95 °C for 30 s, 50 °C for 30 s, 72 °C for 2 min and final extension at 72 °C for 10 min. The PCR amplified 894 base pairs cDNA fragment corresponding to the *Pf*VPS26 gene and pET11a were digested with Nde I and BamH I, and then ligated by T4 DNA Ligase (Thermo Fisher Scientific). The ligation mix was used for transformation in competent DH5α cells followed by their plating on 100 μg/ml carbenicillin containing agar plates. Transformants were screened by colony PCR and positive clones were reconfirmed by restriction digestion. Cloning of *Pf*VPS26 was finally confirmed by gene sequencing.

2.8. PfVPS26 purification

For that, pET11a-*Pf*VPS26 construct was transformed in Rosetta cells which were inoculated in 400 ml of LB broth containing 100 μg/ml carbenicillin plus 40 μg/ml chloramphenicol and grown overnight with shaking at 200 rpm at 37 °C. Next day, LB broth was inoculated with 1% (*v*/v) of overnight grown culture and incubated at 37 °C with shaking at the rate of 200 rpm. The culture was induced with 1 mM IPTG when OD_{600} reached at 0.5–0.6. The culture was further grown for 6 h under same conditions. For purification of *Pf*VPS26, *E. coli* cells overexpressing the protein were harvested by centrifugation at 6000 ×*g* for 5 min followed by lysis in 50 mM Tris HCl buffer with 1% (*w*/*v*) SDS. All the lysate was resolved in 12% SDS-PAGE in batches and the band containing overexpressed *Pf*VPS26 was excised out. *Pf*VPS26 was eluted from the excised bands by electro-elution using Electro-Eluter (Bio-Rad) following the manual given by the manufacturer. The purity of protein was checked on SDS-PAGE and its identity was confirmed by MALDI MS/MS by the procedure described earlier.

2.9. Antibody generation, and co-immunoprecipitation

Polyclonal antibodies against recombinant *Pf*Rab7 and *Pf*VPS26 were generated in 6–8 months old rabbits. Pre-immunization sera were collected and the rabbits were immunized with 0.6 ml pure protein (1 mg/ml concentration) mixed with 0.6 ml of Freund's complete adjuvant (Sigma-Aldrich) by subcutaneous injection of 0.3 ml mixture at 4–5 sites. Three booster doses were given to the rabbits after 2 weeks in a similar way except for Freund's incomplete adjuvant (Sigma-Aldrich) was used this time. Rabbits were bled after 8 weeks through central ear artery. Blood was allowed to clot 4 h at room temperature and kept at 4 °C for overnight. To separate serum, clotted blood was centrifuged at 1000 ×*g* for 30 min and clean pale-yellow serum was collected as supernatant. For IgG purification, Protein-A Mag SepharoseXtra (GE Healthcare) was used following the given protocol. Antibody against *Pf*VPS35 was generated by the protocol as described earlier [39]. Antibodies against *Pf*ERD2, *Pf*Plasmepsin II and *Pf*EBA-175 were obtained from BEI Resources.

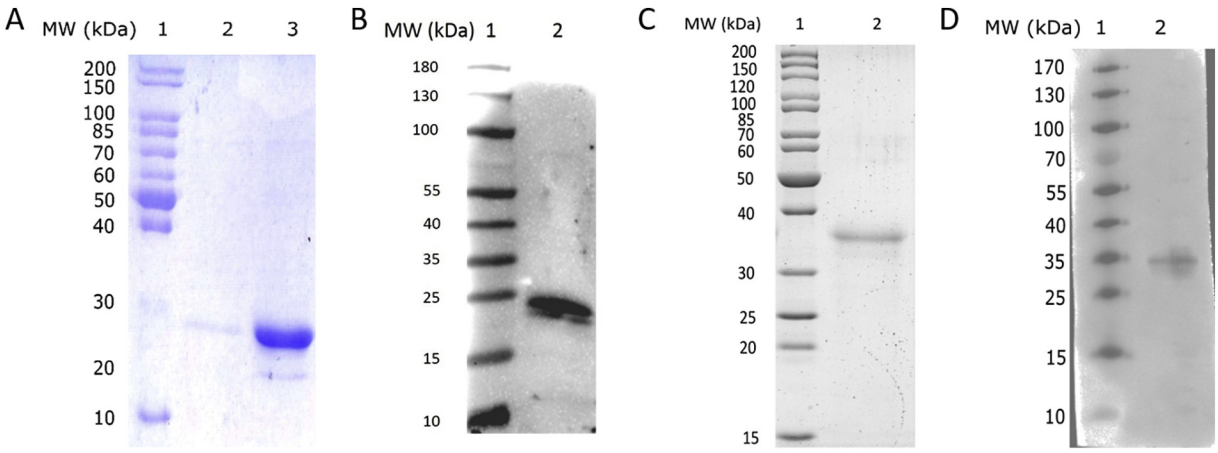

Fig. 1. Recombinant *Pf*Rab7 and *Pf*VPS26 were purified and detected by western blot. (A) The purity of the recombinant *Pf*Rab7 was checked on SDS-PAGE. Lane 2 and 3 show different fractions of eluted recombinant *Pf*Rab7. (B) *Pf*Rab7 was detected by western blot (lane 2) in parasite lysate. (C) The purity of the recombinant *Pf*VPS26 was checked on SDS-PAGE. (D) *Pf*VPS26 was detected by western blot (lane 2) in parasite lysate. MW denotes protein marker (lane 1) with molecular mass in all figures.

Co-IP was performed using Pierce Co-Immunoprecipitation Kit (Thermo Fisher Scientific) as per the given protocol except the parasite cells were lysed in co-IP buffer as described earlier. Since co-IP experiment is very difficult in *P. falciparum* because of very difficult culture conditions, we performed the co-IP in batches using trophozoite enriched culture with approximately 5% parasitemia and the eluted product was pooled before SDS-PAGE and western blot.

2.10. Western blot

Western blotting was performed to check the efficacy of generated antibody and co-IP experiments described earlier [39]. Parasite lysate was used for SDS-PAGE followed by electroblotting on the nitrocellulose membrane. The membrane was blocked by SuperBlock (Thermo Fisher Scientific) for 2 h at room temperature and incubated with primary antibody (anti-*Pf*Rab7 or anti-*Pf*VPS26 or preimmune serum) diluted at 1:1000 dilution in PBS overnight on a shaker at 4 °C. After 3 washings with PBST (PBS with 0.1% Tween-20), membrane was incubated with the HRP-conjugated anti-rabbit secondary antibody (Sigma-Aldrich) at 1:40000 dilution for 2 h at room temperature on a shaker. The membrane was washed thrice with PBST and blots were visualized by ChemiDoc MP Imaging system (Biorad) with Pierce ECL Western Blotting Substrate (Thermo Fisher Scientific). Image Lab 6.0.1 software (Biorad) was used for processing and adjustment of the brightness and contrast of the western blot images.

2.11. Immunofluorescence studies

Infected RBCs were washed with PBS (phosphate buffered saline) and fixed in 4% paraformaldehyde and 0.0075% glutaraldehyde in PBS for 30 min. Fixed cells were washed thrice by PBS and permeabilized with 0.2% Triton X-100 for 30 min at room temperature. Cells were again washed thrice with PBS and treated with 0.1% sodium borohydride for 10 min. Cells were washed 3 times before blocking with SuperBlock (Thermo Fisher Scientific) for 2 h and subsequent incubation with primary antibody (1:200 dilution) in 50% SuperBlock on a shaker at 4 °C overnight. Next day, cells were washed 3 times with PBS followed by incubation with Alexa Fluor conjugated secondary antibodies (Alexa Fluor 488 anti-rabbit and Alexa Fluor 647 anti-mouse, purchased from Thermo Fisher Scientific) in 50% SuperBlock for 2 h at room temperature. Alternately, when the primary antibodies were raised in the same organism, they were chemically linked with fluorophore by protein labelling kit (DyLight488 and DyLight594, from Thermo Fisher Scientific) and directly processed for next step. Cells were mounted on clean glass slides using DAPI containing ProLong Diamond Antifade mounting medium (Thermo Fisher Scientific) and covered with glass coverslips. Antibodies against *Pf*ERD2, *Pf*Plasmepsin II and *Pf*EBA-175 were used as marker for parasite Golgi, DV and microneme. Slides were viewed under a Leica TCS SP8 microscope and all the given images were analyzed and processed by LAS-X software associated with Leica TCS SP8 + SVI Huygens. Deconvolution of the images was performed by SVI Huygens Deconvolution software linked with LAS-X. Approximately 100 cells were screened randomly in different fields and the experiments were repeated twice. Fluorescence signals obtained were given different color for different proteins that may not be the original color for that fluorophore.

2.12. Statistical analysis

All the experiments were performed in triplicates and the images are depicted as representation of three independent experiments. The data were presented as mean ± SEM. The levels of significance were calculated by unpaired Student's *t*-test and one-way analysis of variance using GraphPad Prism 6. P values of < 0.001 were considered significant.

3. Results

3.1. Purification of recombinant PfRab7 and PfVPS26

Multiple sequence of the Rab7 sequence from different species of *Plasmodium* and other representative species revealed significant conservation of the domains (Supplementary Fig. S1). *Pf*Rab7, cloned in pET28a, was overexpressed in *E. coli* and purified by affinity chromatography. On the other hand, *Pf*VPS26 gene was PCR amplified from *P. falciparum* cDNA and cloned in pET11a vector for expression in *E. coli*. Since *Pf*VPS26 was obtained in inclusion bodies, we purified it by electro-elution after resolving the *E. coli* lysate with recombinant *Pf*VPS26 on SDS-PAGE. The proteins were purified to homogeneity and checked on SDS-PAGE for purity (Fig. 1A and C). Purified *Pf*Rab7 and *Pf*VPS26 were checked by MALDI-MS/MS to confirm the identity of the proteins. Their identities were confirmed with a high score (Supplementary Fig. S2A and B). Antibodies raised against the proteins were checked for their specificity by western blot using *E. coli* lysate with recombinant protein and parasite lysate. We found a single band with no visible contaminations in the western blot experiments with both antibodies that confirmed their specificity (Supplementary Fig. S3 and Fig. 1B and D). The recombinant *Pf*Rab7 in *E. coli* was tagged with

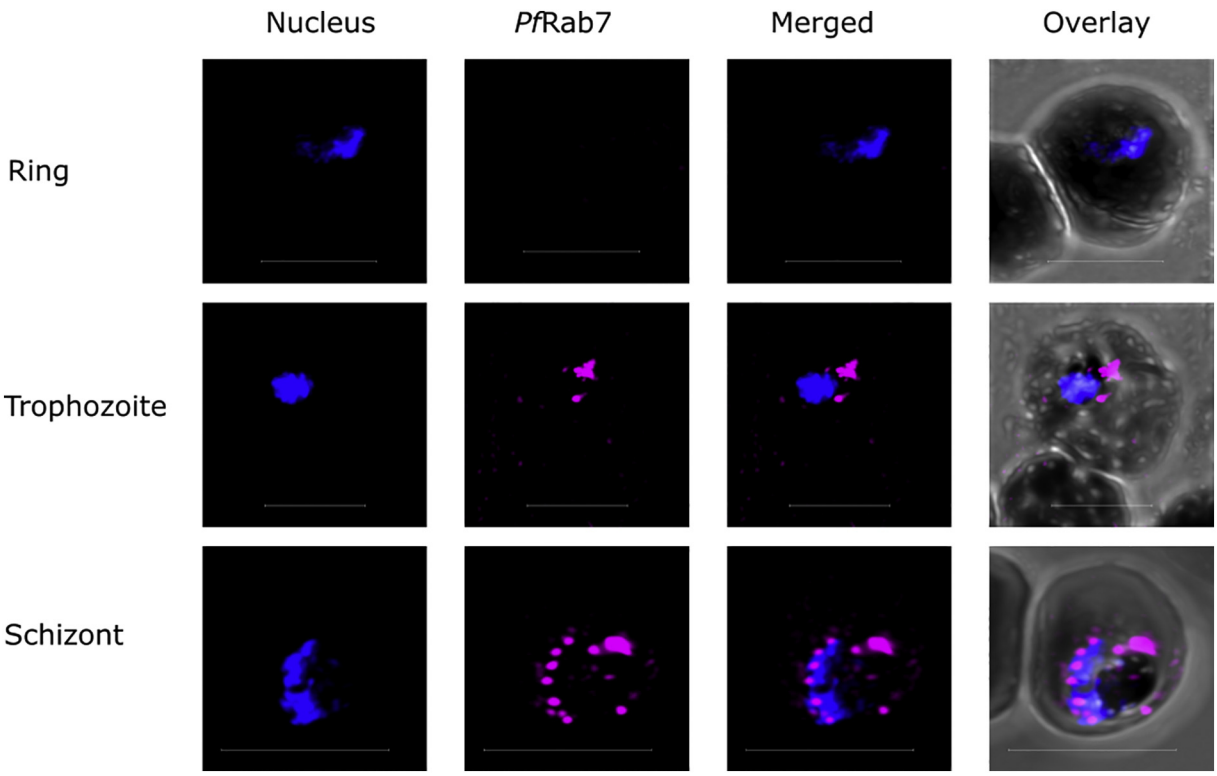

Fig. 2. *Pf*Rab7 appeared as a localized structure in *P. falciparum* trophozoite stage that multiplied in schizont. Parasite was synchronized at ring stage (0 h) and allowed to grow. Infected RBCs were fixed and prepared for confocal microscopy at different time points of growth (ring, trophozoite and schizont). *Pf*Rab7 (magenta) was detected using anti-*Pf*Rab7 antibody followed by anti-rabbit Alexa Fluor 488 and nucleus (blue) was stained by DAPI. Scale bar in each picture indicates 5 μm.

6XHis because of which it appears at higher molecular weight, however, recombinant *Pf*VPS26 does not contain any tag, thus, it appears at similar molecular weight in both parasite and *E. coli*.

3.2. Cellular localization of PfRab7

The location of a protein inside the cell can give crucial information about its cellular function. Therefore, we performed confocal microscopic studies using anti-*Pf*Rab7 antibodies in different intra-erythrocytic stages of the parasite. We found that *Pf*Rab7 was not prominent during ring stage, however, it was found to be condensed at one or two loci during the trophozoite stage (Fig. 2). Further, during the schizont stage, *Pf*Rab7 seems to be distributed among daughter merozoites indicating that the organelle where it is present is inherited by the parasite, unlike other organelles. They further divided and distributed themselves in merozoites as the trophozoites developed into schizonts.

Interestingly, *Pf*Rab7 was found to be localized in the periphery of DV in most of the trophozoites near the black pigment hemozoin, which is a product of heme polymerization produced by the parasite to avoid heme toxicity in its DV. Trophozoite is metabolically most active stage of the parasite when it actively digests host hemoglobin in its DV to support its growth and division. The DV is supported by the cellular machinery to effectively perform its function. Localization of *Pf*Rab7 near DV during trophozoite stage suggested that it might be involved in trafficking from DV, which was regarded as an endolysosomal compartment in the parasite. We checked the localization of *Pf*Rab7 with respect to DV and Golgi markers since the retromer trafficking is known to be directed towards the Golgi. We found that *Pf*Rab7 localized in close association with both DV and Golgi in most of the cells (Fig. 3A and B). We also checked the localization of *Pf*Rab7 with respect to apical organelles in merozoites formed in mature schizonts. We found that *Pf*Rab7 colocalized with *Pf*EBA-175 (Erythrocyte Binding Antigen - 175) at some locations suggesting its possible role related to apical organelles of the parasite (Fig. 3C). To further describe the localization, *Z*-stacking of the cells was also performed to construct a 3-dimensional view of the same cells. Data indicated that *Pf*Rab7 localized in close association with the Golgi and DV based on the confocal studies with anti-*Pf*ERD2 and anti-*Pf*Plasmepsin II antibodies that marked the Golgi and DV, respectively, in most of the trophozoites. There was also some localization with *Pf*EBA-175 at a few loci (Fig. 3D).

3.3. PfRab7 interacted with PfVPS26

Firstly, we performed *in silico* interactome analysis of *Pf*Rab7 and *Pf*VPS26 as a component of retromer complex. It was observed that *Pf*Rab7 interacts with retromer and *vice versa* in *P. falciparum* (Fig. 4A and B). Other proteins predicted to be interacting are listed in Supplementary Table 1. These interacting proteins indicate towards the transportation-related function of *Pf*Rab7. Next, we performed co-IP experiments with anti-*Pf*Rab7 antibody to confirm the observations from previous literature and STRING analysis in *Plasmodium*. A component of retromer complex, *Pf*VPS26 was detected to be interacting with *Pf*Rab7 in parasite lysate that suggested the interaction between retromer complex and *Pf*Rab7 in the parasite. Reverse co-IP was also performed with immobilized anti-*Pf*VPS26 antibody for the detection of *Pf*Rab7 that was pulled out from the parasite lysate. The detection of *Pf*Rab7 and *Pf*VPS26 after co-IP by anti-*Pf*VPS26 and anti-*Pf*Rab7 antibodies, respectively, indicated the physical interaction of these proteins inside the parasite cell (Fig. 4C). We performed co-IP experiment for several times and pooled the eluted product before western blot because co-IP experiments with *P. falciparum* lysate are very difficult to perform. The band of *Pf*VPS26 obtained was very faint that may be due to very low concentration of *Pf*VPS26 present in the cell or less efficiency of the antibody. These data were also supported by a previous study where *Pf*Rab7 was found to be colocalized with another

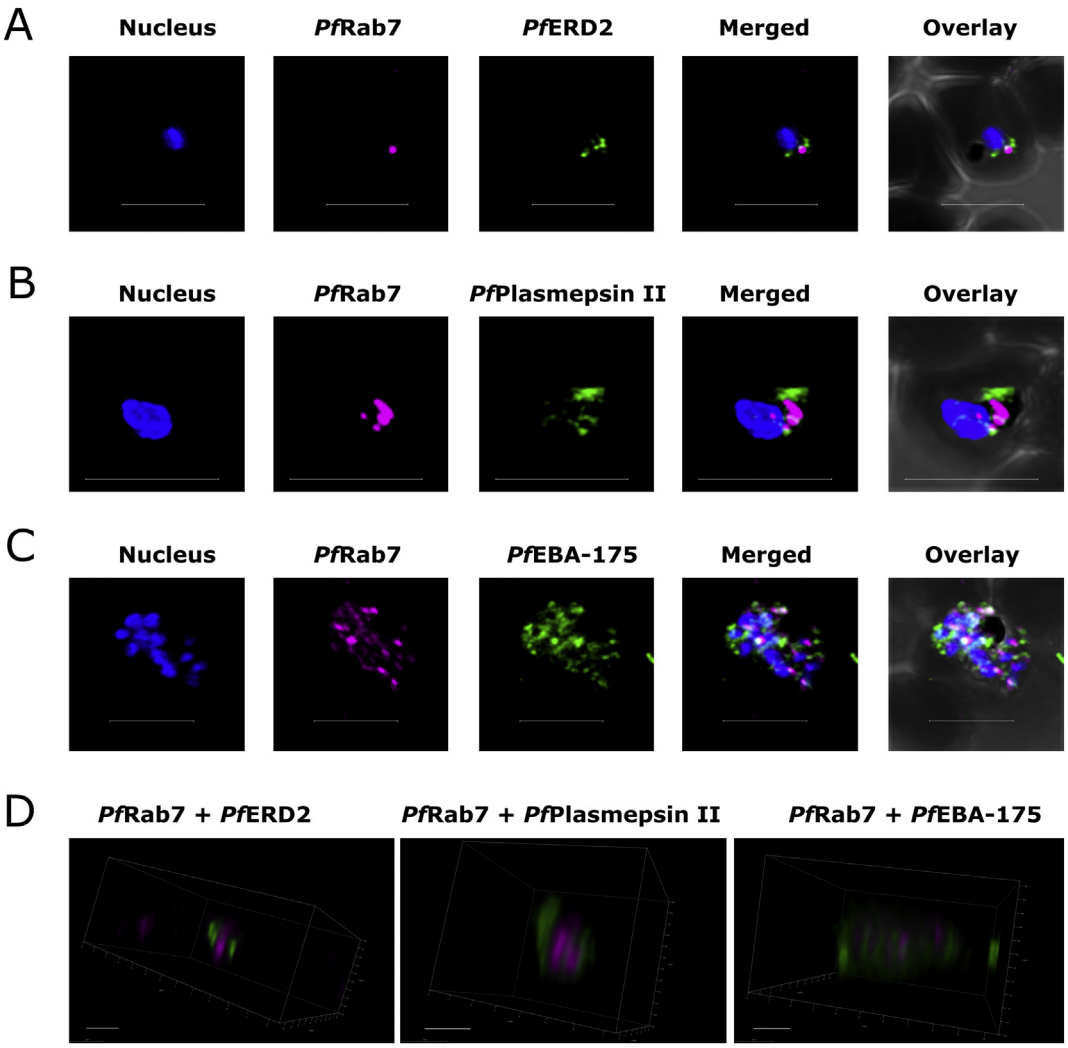

Fig. 3. *Pf*Rab7 was localized near Golgi and DV in most of the trophozoites and at some positions with micronemes. Parasite was immunostained with anti-*Pf*Rab7 antibody and antibodies specific to (A) Golgi, anti-*Pf*ERD2, (B) DV, anti-*Pf*Plasmepsin II and (C) microneme, anti-*Pf*EBA-175. (D) 3-dimensional images captured using *Z*-stacking are presented with indicated combination of the same cells. Scale bar denotes 5 μm in all figures except in 3D view where it denotes 2 μm.

component of the retromer complex, *Pf*VPS35 [26]. We have earlier reported that *Pf*VPS26 and *Pf*VPS35 along with *Pf*VPS29 interact to form retromer complex in the parasite [39]. On the basis of these findings, it can be said that the retromer complex inside parasite interacts with *Pf*Rab7 and functions in a fashion similar to other eukaryotes, granting that the components of the retromer complex are not fully conserved in *Plasmodium*.

3.4. Effect of DV disrupting compounds on the retromer assembly

CQ is a lysosomotropic agent that is selectively taken up by DV where it disrupts heme polymerization [40]. In contrast, atovaquone is known to target mitochondrion of *P. falciparum* [41]. The effect of CQ on the localization of cellular proteins may not be specific and may be due to the killing of parasite, therefore, we treated the parasite with CQ along with atovaquone as a control to check their effects on the distribution of *Pf*Rab7 and *Pf*VPS35 in cell. Data presented that DV disruption by CQ resulted in diffused signals from *Pf*VPS35 indicating the disassembly of retromer complex while there was no apparent effect on *Pf*VPS35 distribution in atovaquone-treated cells (Fig. 5). However, there was no significant change in the distribution of *Pf*Rab7 indicating that its targeting was not affected by CQ. To further validate that DV disruption is causing the retromer dismantling and no other off-target effect of CQ is responsible for that, we needed to perform additional experiments. We synthesized a DV disrupter molecule, compound 5f, which has been earlier shown to inhibit hemozoin formation in the DV of the parasite leading to its disruption and subsequent parasite death [36]. We found that this molecule affected the cellular distribution of *Pf*VPS35 in similar fashion (Fig. 5).

The results obtained by using DV interfering compounds might be a consequence of their antiplasmodial activity. To further ensure the effect of DV disruption on *Pf*Rab7 and *Pf*VPS35 localization, we used a CQ resistant strain K1 of *P. falciparum*. Here we found that the effect of CQ was diminished while compound 5f had similar effects on the distribution of *Pf*VPS35 (Fig. 6). The data showed that interfering with DV resulted in the dismantling of the retromer complex that may be due to the inhibition of *Pf*Rab7 that might be the controller of the retromer complex. The concentrations of the compound that were used were not able to adversely affect the morphology of the parasite and the parasite was able to grow after removal of the compound.

3.5. PfRab7 was predicted to contain GTPase domain

*Pf*Rab7 structure was modelled using *in silico* approach. We employed I-TASSER, a three-dimensional structure prediction web server for proteins with *ab initio* methodology, to predict the structure of *Pf*Rab7 with a confidence score of 0.92 (Fig. 7A). It was found to be similar to mammalian Rab7 with the conserved catalytic domain.

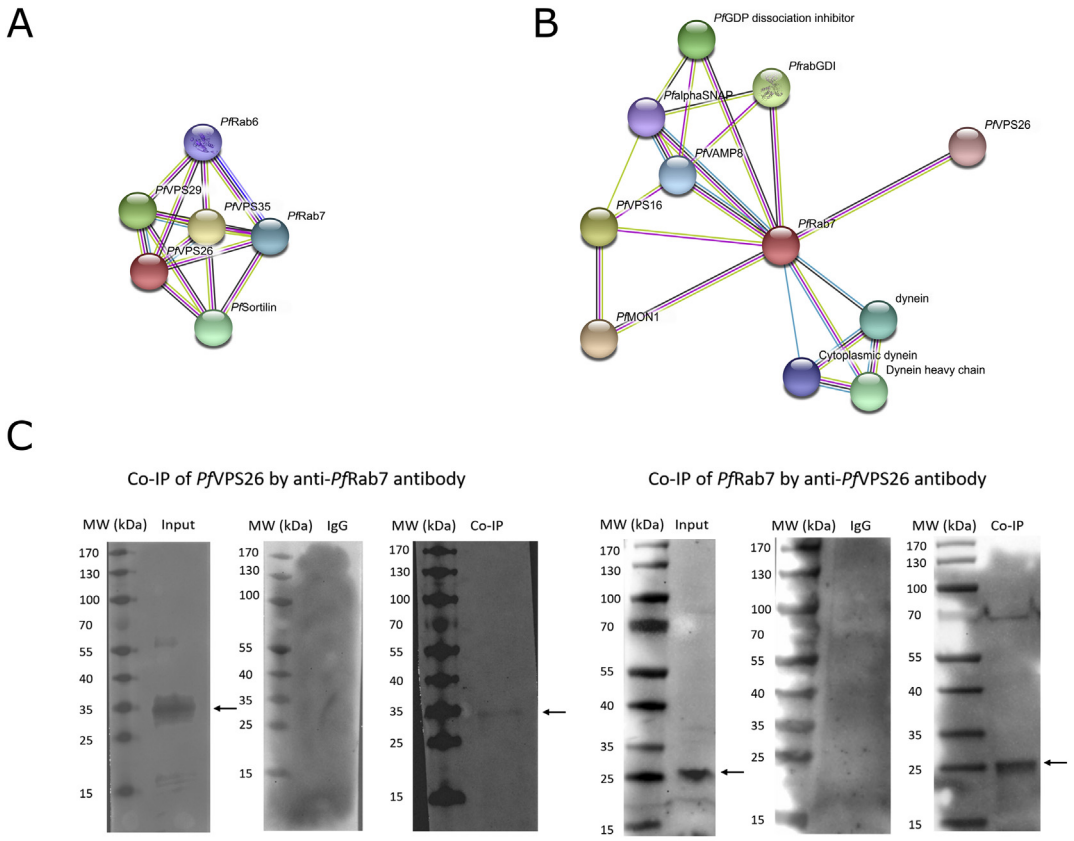

Fig. 4. *Pf*Rab7 was predicted to interact with *Pf*VPS26; that was confirmed by coimmunoprecipitation experiments. Interacting proteins with *Pf*VPS26 (A) and *Pf*Rab7 (B) were predicted by STRING database with minimum confidence score of 0.7. (C) Immunodetection of *Pf*VPS26 and *Pf*Rab7 by Co-IP using anti-*Pf*Rab7 and anti-*Pf*VPS26 antibodies, respectively. Control experiments are shown with IgG and input parasite lysate.

Conserved GTP and divalent magnesium binding sites were also predicted in the structure and sequence of *Pf*Rab7 (Fig. 7B). Predicted structure of *Pf*Rab7 showed close resemblance to YPT1 (Fig. 7C). Glycine and glutamine at 18th and 67th positions, respectively, were predicted to be conserved in *Pf*Rab7 (Fig. 7D). Bioinformatics provided some crucial information about *Pf*Rab7 that further needed to be validated using purified *Pf*Rab7.

3.6. PfRab7 GTPase activity was inhibited by CID 1067700 that checked parasite growth

We checked the purified *Pf*Rab7 for its GTPase activity. Rab proteins have slow intrinsic GTPase activity [42] that has been observed in mammalian Rab7 as well [43]. The GTPase activity of *Pf*Rab7 was observed, and its K_m was found to be 0.18 ± 0.02 mM with V_{max} 25.95 ± 0.75 μM/min (Fig. 8A). Upon further calculation the catalytic rate constant, k_{cat} of the protein was found to be 1.6 ± 0.05/min. The GTPase activity of Rab7 has been reported to be inhibited by CID 1067700, which specifically inhibits its GTPase activity by binding competitively to its nucleotide binding pocket [44]. *Pf*Rab7 share significant homology and structural similarity with its mammalian counterparts with conserved enzymatic site (Supplementary Fig. S1 and Fig. 7). This prompted us to evaluate the effect of CID 1067700 treatment on the GTPase activity of recombinant *Pf*Rab7. Therefore, we tested this compound for its effects on the intrinsic GTPase activity of *Pf*Rab7 by estimation of inorganic phosphate released upon enzymatic hydrolysis of GTP.

We found that CID 1067700 concentration-dependently inhibited the GTPase activity of *Pf*Rab7 (Fig. 8B). Another GTPase inhibitor dynasore hydrate was taken as control which did not inhibit *Pf*Rab7 GTPase activity. This indicated that GTPase activity of *Pf*Rab7 was inhibited by Rab7 specific inhibitor CID 1067700. This provided a chemical tool to investigate the Rab7 regulated protein trafficking pathway in a unique cellular set up like *Plasmodium*. We further employed chemical inhibitor of *Pf*Rab7 to investigate its role with respect to retrograde trafficking in *Plasmodium*. The GTPase activity of Rab7 is dependent on the divalent metal ion, magnesium [43] and *Pf*Rab7 was also predicted to be containing a divalent magnesium biding site. We, therefore, performed GTPase assay of *Pf*Rab7 in absence of magnesium and presence of increasing concentrations of metal ion chelator, EDTA. Data indicated that removal of magnesium hampered the GTPase activity of *Pf*Rab7 (Fig. 8C). We performed another experiment by using Rab7 inhibitor CID 1067700 to check its effects on the localization of *Pf*VPS35 whose assembly was suggested to be regulated by *Pf*Rab7. We found that CID 1067700 affected the localization pattern of *Pf*VPS35 that resulted in diffused signals (Fig. 8D). Data demonstrated that the inhibition of *Pf*Rab7 resulted in the disassembly of retromer complex. This further indicated the possible role of *Pf*Rab7 as a regulator retromer complex in *P. falciparum*. CID 1067700 also inhibited parasite growth and its inhibitory concentration (IC_{50}) was found to be 12.87 ± 0.9 μM as measured by SYBR Green assay. Upon further investigation after its treatment using microscopy, the morphology of the parasite appeared distorted and damaged indicating the death of the parasite (Fig. 9A and B).

4. Discussion

Plasmodium, during its evolution, developed unique organelles like DV and apicoplast for its survival. To describe the functions of these unique organelles which are absent in other well-defined eukaryotic cells, intracellular protein trafficking in *Plasmodium* needs to be thoroughly investigated. This study provides insights into the Rab7 and

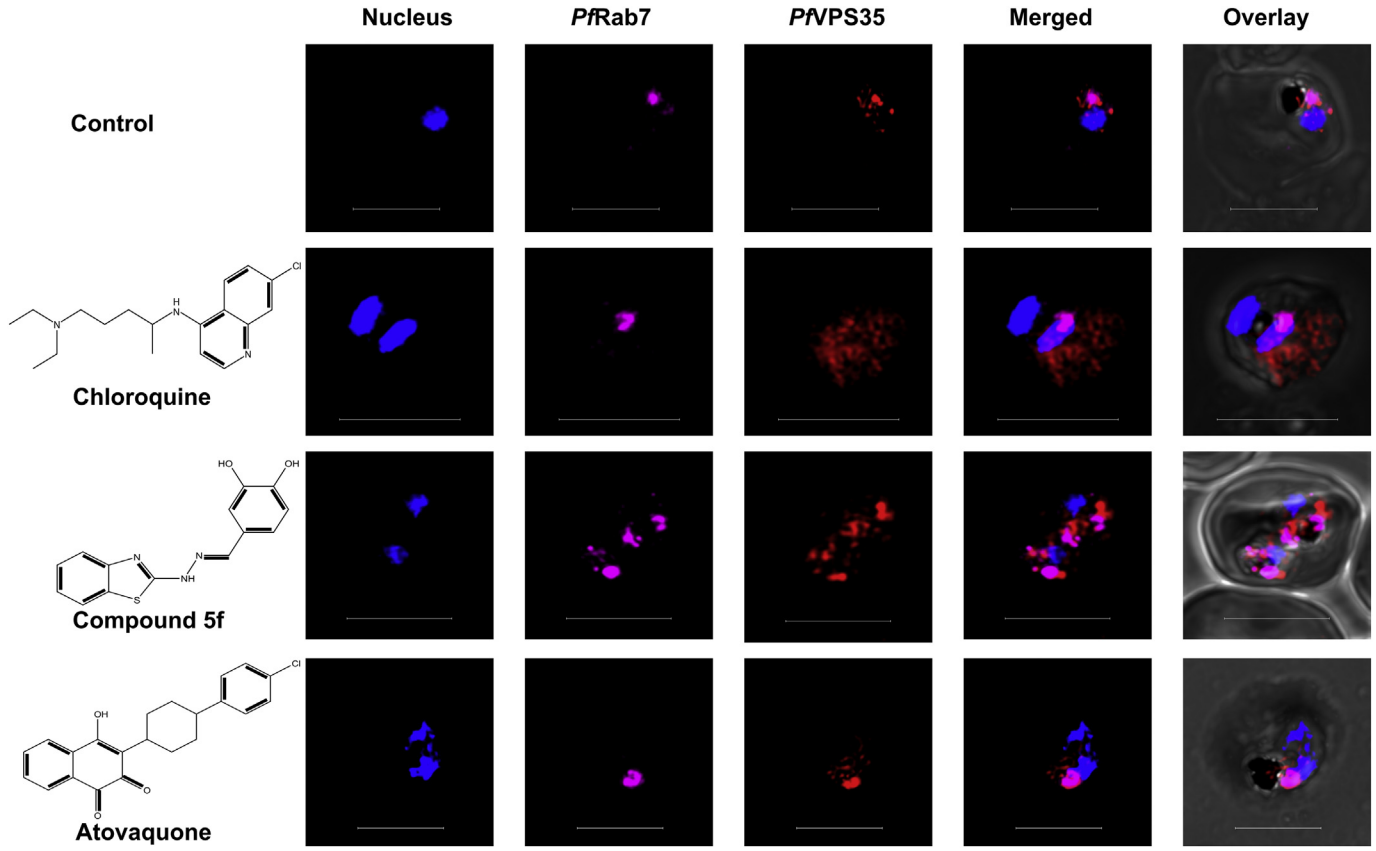

Fig. 5. Distribution of *Pf*VPS35 upon chloroquine and compound 5f treatment in *P. falciparum* 3D7 strain. Parasite was treated with different compounds as described in Materials and Methods followed by fixing and immunostaining of *Pf*Rab7 and *Pf*VPS35. Scale bar in each picture indicates 5 μm.

retromer complex assembly in *P. falciparum*. Although the localization of *Pf*Rab7 and retromer complex near DV was visible near black pigment, it was further validated by using a DV marker, *Pf*Plasmepsin II. Similarly, for Golgi, its marker *Pf*ERD2 was used which has been shown to colocalize with a known Golgi protein, Golgi re-assembly stacking protein (*Pf*GRASP) in parasite [45,46]. In a recent report, *Pf*Sortilin was reported to be involved in trafficking to another apical organelle, rhoptries, in merozoites [47]. Sortilin has been reported as an interacting protein of the retromer complex in *P. falciparum* and *Toxoplasma gondii* [39,48]. Thus, it can be suggested that the *Pf*Rab7 might regulate

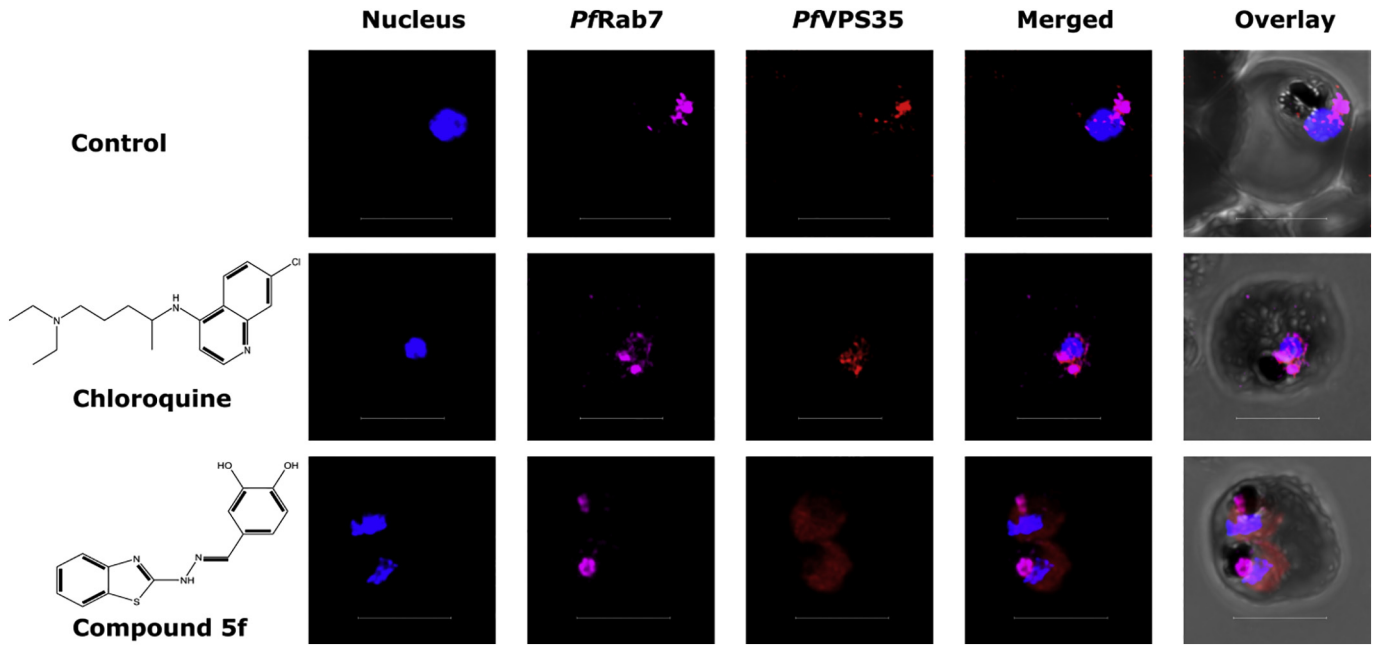

Fig. 6. Distribution of *Pf*VPS35 upon compound 5f treatment in *P. falciparum* K1 strain where chloroquine was ineffective. Parasite was treated with CQ and compound 5f as described in Materials and Methods followed by fixing and immunostaining of *Pf*Rab7 and *Pf*VPS35. Scale bar in each picture indicates 5 μm.

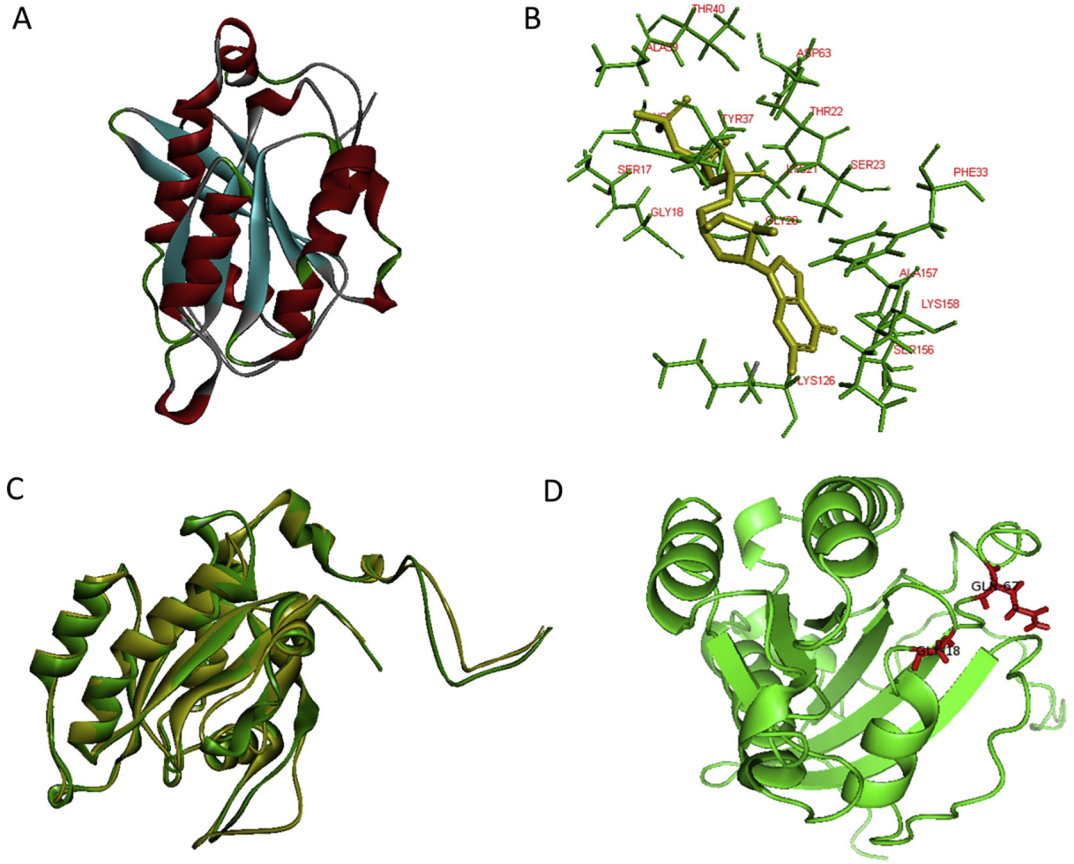

Fig. 7. Structure prediction of *Pf*Rab7 by I-TASSER. (A) Structure of *Pf*Rab7 as predicted by I-TASSER showing identified β-sheets (cyan) and α-helices (red). (B) Figure depicting predicted amino acids of *Pf*Rab7 forming the GTP binding fold (green) with GTP molecule (yellow) in the center. (C) Alignment of *Pf*Rab7 structure with YPT1 GTPase showing close resemblance. *Pf*Rab7 is shown in green color and YPT1 in yellow color. (D) Predicted enzymatic site in *Pf*Rab7 with conserved amino acids (glycine 18 and glutamine 67) are shown in red color.

the retrograde trafficking of proteins from the DV to the Golgi in *P. falciparum*.

To explore the function of *Pf*Rab7 in the parasite, we needed to obtain the constituent proteins in purified form for their molecular characterization. We began with the sequence analysis of *Pf*Rab7. Many conserved proteins have been identified in the *Plasmodium* genome and curated at PlasmoDB [49]. Rab-interactome of *Plasmodium* with respect to *Saccharomyces* has been described earlier where *Pf*Rab7 was found to be a homolog of Ypt7 and cAMP-dependent protein kinase A was found to be its effector protein in parasite [50]. There are more than 10 Rab proteins found to be conserved in *Plasmodium* genome [51]. Sequence analysis suggests the similar function of the protein in the parasite; however, the functional and structural distinctiveness of the *Plasmodium* cell raises interesting questions about the functioning of *Pf*Rab7. *Pf*Rab7 contains a conserved lysine at 158 position that directs towards its possible interaction with retromer complex [52]. *P. falciparum* also contains several conserved cysteine residues. Two cysteine residues at the carboxy terminal of the protein pointed to the prenylation of *Pf*Rab7. Proteomic analysis of all proteins in *P. falciparum* that got prenylated included *Pf*Rab7 [53]. Moreover, the conservation of two consecutive cysteine residues 83 and 84 in *Pf*Rab7 indicated that its palmitoylation was essential for endosome to Golgi trafficking as reported earlier [54], however, *Pf*Rab7 was not found to be palmitoylated when over 400 palmitoylated protein of *P. falciparum* were analyzed [55]. After sequence analysis, *Pf*Rab7 was overexpressed and purified to homogeneity and subjected to MALDI MS/MS analysis to confirm its identity and antibody generation. Rab7, in mammalian cells, is known to regulate the retromer trafficking, therefore, we also cloned, overexpressed and purified *Pf*VPS26, a structural component of retromer complex of *P. falciparum*. Antibodies were generated against both recombinant proteins and validated by western blot using parasite lysate. We obtained very specific antibodies against both proteins as evident by single band after western blot with parasite lysate. During immunofluorescence studies, *Pf*Rab7 was mostly found to be localized in the vicinity of DV and the Golgi. Next, to assess the interaction of *Pf*Rab7 with retromer complex in *P. falciparum*, we performed co-IP experiments. In spite of difficult culture conditions and low yield of parasite lysate that make such studies formidable, we were able to pull down *Pf*VPS26 using anti-*Pf*Rab7 antibody and *vice-versa*. The interaction between *Pf*Rab7 and retromer complex suggested the regulation of retromer movement by *Pf*Rab7 in *P. falciparum* which is in agreement to a previous report where retromer assembly and VPS26 interaction with Rab7 was shown in another apicomplexan parasite *Toxoplasma gondii* near its endosome-like compartment [56]. To further confirm the role of *Pf*Rab7 as a regulator of retromer assembly, genetic manipulation of active site of *Pf*Rab7 may be performed that is extremely difficult in *P. falciparum* because it may be harmful for its growth and difficulty in transfection experiments with parasite [51,57]. Next, due to gathering of *Pf*Rab7 in vicinity of DV, we intended to check the effects of DV disruption on *Pf*Rab7 function that is retromer trafficking using CQ. The treatment of CQ on retromer movement revealed that the retrograde trafficking depends on the proper functioning of DV since CQ is known to be a disrupter of DV while atovaquone that targets mitochondrion did not show such effects. This observation was further supported by the use of another DV disrupter compound 5f. Earlier coumarin labelled-CQ has been shown to permeabilize DV at 30 μM which indicates physical disruption of DV by fluorescence microscopy [58], however, in a different study CQ was shown to inhibit endocytosis in *Plasmodium* at

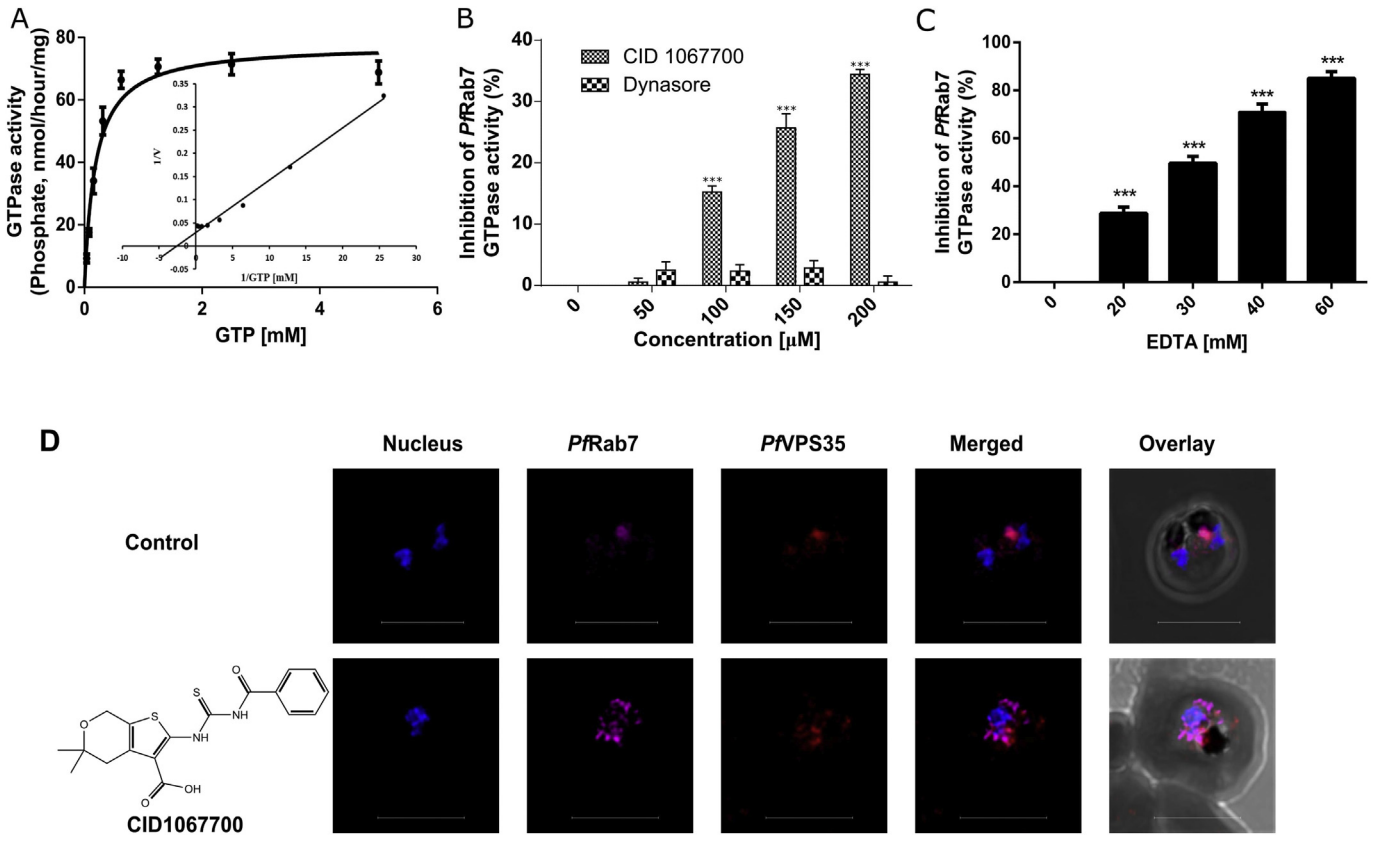

Fig. 8. Characterization of *Pf*Rab7 GTPase activity. (A) GTPase activity of *Pf*Rab7 determined by plotting the amount of phosphate released against different concentrations of substrate GTP. Data represent Mean ± SEM. (B) Effect of CID 1067700 and dynasore on GTPase activity of *Pf*Rab7 at different concentrations of the compounds. (C) Effect of different concentrations of divalent ion chelator EDTA on the GTPase activity of *Pf*Rab7. The experiment was performed in triplicate. Data are shown as means ± SEM (***$P < .001$ [*versus* the control]). (D) The localization of *Pf*Rab7 and *Pf*VPS35 in presence of CID 1067700 (10 μM). Scale bar in each picture indicates 5 μm.

120 nM [59]. This indicates that CQ at low concentrations can affect the physiological functions in the parasite and physically disrupt it at higher concentrations. Interestingly, in a similar experiment on CQ resistant *P. falciparum* K1 strain, CQ was found to be ineffective while compound 5f showed the same result. This indicated that the CQ and compound 5f acted specifically on the DV that led to the dismantling of the retromer complex. It was observed that there was not much effect of CQ treatment on the localization of *Pf*Rab7 that may be because of various other functions of *Pf*Rab7 where it was not dependent on the DV, like its role in autophagy like process in the parasite [60].

Structure prediction tools gave clues about conserved GTPase site in *Pf*Rab7 as previously identified [26]. The indications given by bioinformatics tools were not sufficient to draw any interpretation. Based on these observations, we performed additional experiments to further characterize the role of *Pf*Rab7 in *P. falciparum*. The GTPase activity is crucial for the biological functions of Rab7 [61]. Therefore, recombinant *Pf*Rab7 was subjected to further biochemical studies. Enzyme kinetics and inhibition studies for the GTPase activity of *Pf*Rab7 indicated towards its conserved function in the cell. This also provided a chemical tool to study its role in the parasite. Next, we needed to assess the loss of *Pf*Rab7 function on retromer assembly in parasite cell. Thus, we treated the parasite with CID 1067700 and checked the cellular localization of *Pf*Rab7 and *Pf*VPS35. The concentration and time for CID 1067700 treatment were chosen after testing different

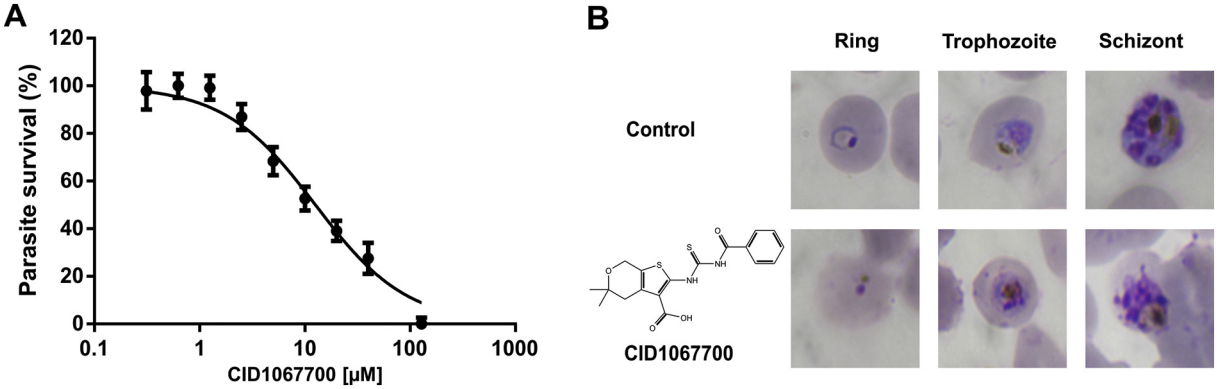

Fig. 9. Inhibition of *P. falciparum* growth by CID 1067700. (A) IC_{50} of CID 1067700 was calculated by non-linear regression curve using GraphPad Prism. Data represent Mean ± SEM. (B) Effect of CID 1067700 (10 μM) on parasite morphology.

concentrations and time points. At 10 μM, CID 1067700 did not affect the morphology of the cell and in a previous report its treatment at 5 μM inhibited the autophagy related function of Rab7 in mammalian cells [62]. Data indicated that CID 1067700 inhibited the GTPase activity of recombinant *Pf*Rab7 at 200 μM and in parasite culture, it resulted in diffused localization of both *Pf*Rab7 and *Pf*VPS35 at 10 μM. CID 1067700 treatment at 12.87 ± 0.9 μM concentration led to the inhibition of parasite growth. Although CID 1067700 inhibited enzymatic activity of recombinant *Pf*Rab7 at higher concentrations, it inhibited the parasite growth at lower concentration. This might be due to the localized accumulation of CID 1067700 in the cell even with low concentration in the culture media and the possibility of some off-targets effect of CID 1067700 cannot be ignored. Antiplasmodial activity of this compound at low concentration can also be due to long incubation period of 48 h in the IC_{50} calculation experiment.

Sequence similarity of *Pf*Rab7 with other eukaryotic homologs pointed to the similar function but the distinct cellular architecture of *P. falciparum* and lack of homologs of structural sub-complex of retromer that are SNX1/SNX2 and SNX5/SNX6, contradict the given paradigm. Also, it does not contain any well-defined classical eukaryotic endosome-lysosome system. Thus, it raises interesting questions about the endocytic protein trafficking pathways in *Plasmodium*. In this study, we attempted to functionally characterize *Pf*Rab7 with respect to retromer complex assembly. We presented the physical interaction between *Pf*Rab7 and retromer complex which suggested the regulation of retromer assembly as a function of *Pf*Rab7 in *Plasmodium*. Effect of the Rab7 inhibitor on *Pf*Rab7 and *Pf*VPS35 distribution in parasite further validated this function of *Pf*Rab7.

DV is a crucial component of endocytic pathways in *Plasmodium* that is supported by the targeting of endocytosis related proteins such as *Pf*Rab5B to the DV [63]. Here we report the association of *Pf*Rab7 with DV through confocal microscopy that was also supported by proteomics analysis of DV conducted in another study [64]. Rab7 has been found to be important for the biogenesis of lysosome [65]. On that basis, its role in the biogenesis of *Plasmodium* DV can be investigated. Another role of *Pf*Rab7 has been reported in autophagy where it was reported to associate with *Pf*ATG8 around the DV during starvation condition [60]. All these evidences describe the significance of *Pf*Rab7 in *Plasmodium* which is supported by the inability to generate Rab7 knock out parasite in *P. berghei* [50,51]. The data obtained in this study provides crucial insights about the functioning of *Pf*Rab7 as a possible regulator of retromer assembly in parasite that can be explored as a drug target. Secondly, the close association of retromer trafficking with the DV of *P. falciparum* shown in this study provided more details about the role of this organelle in the physiology of the parasite.

5. Conclusion

The present study explores the role of *Pf*Rab7 and its interaction with the retromer complex in *P. falciparum*. Gathering of *Pf*Rab7 and *Pf*VPS35 in vicinity of DV and Golgi indicated towards the trafficking of retromer complex between these organelles in the parasite. The DV targeting compounds, CQ and compound 5f, dismantled the retromer assembly near DV which indicated that proper DV functioning is crucial for the retromer trafficking in the parasite. The results were further validated by using CQ-resistant strain of *P. falciparum* where CQ was unable to show any effect, however, compound 5f exhibited similar effects. *Pf*Rab7 GTPase was, further, characterized biochemically and shown to be inhibited by CID 1067700. This compound also resulted in the delocalization of *Pf*Rab7 and *Pf*VPS35 and suppression of parasite growth. In brief, in the present work, we showed the interaction of retromer complex in *P. falciparum* with *Pf*Rab7, the location of its assembly in the parasite and the involvement of DV in retromer trafficking.

Ethics statement

The antibodies were generated in the rabbit. All animals were obtained from the animal house of CSIR-Indian Institute of Chemical Biology, Kolkata. Animal handling and other experimental procedures were conducted in agreement with the regulations of Institutional Animal Ethics Committee (IAEC) and Committee for the Purpose of Control and Supervision of Experiments on Animals (CPCSEA, Permit Number: 147/1999/CPCSEA).

Declaration of competing interest

The authors declare no conflict of interest associated with this publication.

Acknowledgment

This study was supported by the Council of Scientific and Industrial Research (CSIR), New Delhi, through grants (SPlenDID, BSC 0104). We also thank CSIR for providing fellowship to Asim Azhar Siddiqui. We acknowledge the financial support from DST (J. C. Bose Fellowship, SB/S2/JCB-54/2014). We are thankful to Mr. Saunak Bhattacharya (Technical Officer at CSIR - IICB) for his help in confocal microscopy. The following reagents were obtained through BEI Resources, NIAID, NIH: Polyclonal Anti-*Plasmodium falciparum Pf*ERD2 (antiserum, Rabbit), contributed by John H. Adams, Polyclonal Anti-*Plasmodium falciparum* Plasmepsin II (antiserum, Rabbit), MRA-66, contributed by Daniel E. Goldberg and Monoclonal Antibody R217 Anti-*Plasmodium falciparum* 175 kDa Erythrocyte Binding Antigen (EBA-175), Region II, F2 Domain, MRA-711A, contributed by EntreMed/NIAID.

Appendix A. Supplementary data

Supplementary data to this article can be found online at https://doi.org/10.1016/j.bbagen.2020.129656.

References

[1] D.E. Goldberg, A.F. Slater, A. Cerami, G.B. Henderson, Hemoglobin degradation in the malaria parasite Plasmodium falciparum: an ordered process in a unique organelle, Proc. Natl. Acad. Sci. U. S. A. 87 (1990) 2931–2935, https://doi.org/10.1073/PNAS.87.8.2931.

[2] P.L. Olliaro, D.E. Goldberg, The *Plasmodium* digestive vacuole: metabolic headquarters and choice drug target, Parasitol. Today 11 (1995) 294–297, https://doi.org/10.1016/0169-4758(95)80042-5.

[3] A. Alam, M. Goyal, M.S. Iqbal, C. Pal, S. Dey, S. Bindu, P. Maity, U. Bandyopadhyay, Novel antimalarial drug targets: hope for new antimalarial drugs, Expert. Rev. Clin. Pharmacol. 2 (2009) 469–489, https://doi.org/10.1586/ecp.09.28.

[4] U. Bandyopadhyay, S. Dey, Antimalarial drugs and molecules inhibiting hemozoin formation, Apicomplexan Parasites, Wiley-VCH Verlag GmbH & Co. KGaA, Weinheim, Germany, 2011, pp. 205–234, , https://doi.org/10.1002/9783527633883.ch11.

[5] A.B. Vaidya, M.W. Mather, Mitochondrial evolution and functions in malaria parasites, Annu. Rev. Microbiol. 63 (2009) 249–267, https://doi.org/10.1146/annurev.micro.091208.073424.

[6] S. Sun, L. Lv, Z. Yao, P. Bhanot, J. Hu, Q. Wang, Identification of endoplasmic reticulum-shaping proteins in *Plasmodium* parasites, Protein Cell 7 (2016) 615–620, https://doi.org/10.1007/s13238-016-0290-5.

[7] N.S. Struck, S. Herrmann, I. Schmuck-Barkmann, S. de Souza Dias, S. Haase, A.L. Cabrera, M. Treeck, C. Bruns, C. Langer, A.F. Cowman, M. Marti, T. Spielmann, T.W. Gilberger, Spatial dissection of the cis- and trans-Golgi compartments in the malaria parasite *Plasmodium falciparum*, Mol. Microbiol. 67 (2008) 1320–1330, https://doi.org/10.1111/j.1365-2958.2008.06125.x.

[8] P.J. Rosenthal, Cysteine proteases of malaria parasites, Int. J. Parasitol. 34 (2004) 1489–1499, https://doi.org/10.1016/j.ijpara.2004.10.003.

[9] S.E. Francis, D.J. Sullivan, D.E. Goldberg, Hemoglobin metabolism in the malaria parasite *Plasmodium falciparum*, Annu. Rev. Microbiol. 51 (1997) 97–123, https://doi.org/10.1146/annurev.micro.51.1.97.

[10] K.J. Milani, T.G. Schneider, T.F. Taraschi, Defining the morphology and mechanism of the hemoglobin transport pathway in *Plasmodium falciparum*-infected erythrocytes, Eukaryot. Cell 14 (2015) 415–426, https://doi.org/10.1128/EC.00267-14.

[11] N. Abu Bakar, N. Klonis, E. Hanssen, C. Chan, L. Tilley, Digestive-vacuole genesis and endocytic processes in the early intraerythrocytic stages of *Plasmodium*

falciparum, J. Cell Sci. 123 (2010) 441–450, https://doi.org/10.1242/jcs.061499.
[12] M. Deponte, H.C. Hoppe, M.C.S. Lee, A.G. Maier, D. Richard, M. Rug, T. Spielmann, J.M. Przyborski, Wherever I may roam: protein and membrane trafficking in *P. falciparum*-infected red blood cells, Mol. Biochem. Parasitol. 186 (2012) 95–116, https://doi.org/10.1016/j.molbiopara.2012.09.007.
[13] D.A. Elliott, M.T. McIntosh, H.D. Hosgood, S. Chen, G. Zhang, P. Baevova, K.A. Joiner, Four distinct pathways of hemoglobin uptake in the malaria parasite *Plasmodium falciparum*, Proc. Natl. Acad. Sci. U. S. A. 105 (2008) 2463–2468, https://doi.org/10.1073/pnas.0711067105.
[14] A.H. Hutagalung, P.J. Novick, Role of Rab GTPases in membrane traffic and cell physiology, Physiol. Rev. 91 (2011) 119–149, https://doi.org/10.1152/physrev.00059.2009.
[15] K. Wennerberg, K.L. Rossman, C.J. Der, The Ras superfamily at a glance, J. Cell Sci. 118 (2005) 843–846, https://doi.org/10.1242/jcs.01660.
[16] Y. Zhen, H. Stenmark, Cellular functions of Rab GTPases at a glance, J. Cell Sci. 128 (2015) 3171–3176, https://doi.org/10.1242/jcs.166074.
[17] M. Zerial, H. McBride, Rab proteins as membrane organizers, Nat. Rev. Mol. Cell Biol. 2 (2001) 107–117, https://doi.org/10.1038/35052055.
[18] M.-T.G. Lee, A. Mishra, D.G. Lambright, Structural mechanisms for regulation of membrane traffic by rab GTPases, Traffic (Copenhagen, Denmark). 10 (2009) 1377–1389, https://doi.org/10.1111/j.1600-0854.2009.00942.x.
[19] K.F. Leung, R. Baron, M.C. Seabra, Thematic review series: lipid posttranslational modifications. Geranylgeranylation of Rab GTPases, J. Lipid Res. 47 (2006) 467–475, https://doi.org/10.1194/jlr.R500017-JLR200.
[20] P. Chavrier, R.G. Parton, H.P. Hauri, K. Simons, M. Zerial, Localization of low molecular weight GTP binding proteins to exocytic and endocytic compartments, Cell 62 (1990) 317–329, https://doi.org/10.1016/0092-8674(90)90369-P.
[21] R. Jambou, A. Zahraoui, B. Olofsson, A. Tavitian, G. Jaureguiberry, Small GTP-binding proteins in Plasmodium falciparum, Biol. Cell. 88 (1996) 113–121, https://doi.org/10.1111/j.1768-322X.1996.tb00985.x.
[22] A. Priya, I.V. Kalaidzidis, Y. Kalaidzidis, D. Lambright, S. Datta, Molecular insights into Rab7-mediated endosomal recruitment of core retromer: deciphering the role of Vps26 and Vps35, Traffic (Copenhagen, Denmark) 16 (2015) 68–84, https://doi.org/10.1111/tra.12237.
[23] R. Rojas, T. van Vlijmen, G.A. Mardones, Y. Prabhu, A.L. Rojas, S. Mohammed, A.J.R. Heck, G. Raposo, P. van der Sluijs, J.S. Bonifacino, Regulation of retromer recruitment to endosomes by sequential action of Rab5 and Rab7, J. Cell Biol. 183 (2008) 513–526, https://doi.org/10.1083/jcb.200804048.
[24] L.K. Purushothaman, H. Arlt, A. Kuhlee, S. Raunser, C. Ungermann, Retromer-driven membrane tubulation separates endosomal recycling from Rab7/Ypt7-dependent fusion, Mol. Biol. Cell 28 (2017) 783–791, https://doi.org/10.1091/mbc.e16-08-0582.
[25] T.-T. Liu, T.S. Gomez, B.K. Sackey, D.D. Billadeau, C.G. Burd, Rab GTPase regulation of retromer-mediated cargo export during endosome maturation, Mol. Biol. Cell 23 (2012) 2505–2515, https://doi.org/10.1091/mbc.e11-11-0915.
[26] P. Krai, S. Dalal, M. Klemba, Evidence for a Golgi-to-endosome protein sorting pathway in Plasmodium falciparum, PLoS One 9 (2014), https://doi.org/10.1371/journal.pone.0089771 e89771.
[27] C. Burd, P.J. Cullen, Retromer: a master conductor of endosome sorting, Cold Spring Harb. Perspect. Biol. 6 (2014), https://doi.org/10.1101/cshperspect.a016774 a016774.
[28] M. Gallon, P.J. Cullen, Retromer and sorting nexins in endosomal sorting, Biochem. Soc. Trans. 43 (2015) 33–47, https://doi.org/10.1042/BST20140290.
[29] A.S. Mukadam, M.N.J. Seaman, Retromer-mediated endosomal protein sorting: the role of unstructured domains, FEBS Lett. 589 (2015) 2620–2626, https://doi.org/10.1016/j.febslet.2015.05.052.
[30] K.-E. Chen, M.D. Healy, B.M. Collins, Towards a molecular understanding of endosomal trafficking by Retromer and Retriever, Traffic 20 (2019) 465–478, https://doi.org/10.1111/tra.12649.
[31] Y. Zhang, I-TASSER: fully automated protein structure prediction in CASP8, Proteins 77 (2009) 100–113, https://doi.org/10.1002/prot.22588.
[32] J. Yang, Y. Zhang, I-TASSER server: new development for protein structure and function predictions, Nucleic Acids Res. 43 (2015) W174–W181, https://doi.org/10.1093/nar/gkv342.
[33] A. Alam, M. Goyal, M.S. Iqbal, S. Bindu, S. Dey, C. Pal, P. Maity, N.M. Mascarenhas, N. Ghoshal, U. Bandyopadhyay, Cysteine-3 and cysteine-4 are essential for the thioredoxin-like oxidoreductase and antioxidant activities of *Plasmodium falciparum* macrophage migration inhibitory factor, Free Radic. Biol. Med. 50 (2011) 1659–1668, https://doi.org/10.1016/j.freeradbiomed.2011.03.012.
[34] M.S. Iqbal, A.A. Siddiqui, A. Alam, M. Goyal, C. Banerjee, S. Sarkar, S. Mazumder, R. De, S. Nag, S.J. Saha, U. Bandyopadhyay, Expression, purification and characterization of *Plasmodium falciparum* vacuolar protein sorting 29, Protein Expr. Purif. 120 (2016) 7–15, https://doi.org/10.1016/j.pep.2015.12.004.
[35] V. Dery, N.O. Duah, R. Ayanful-Torgby, S.A. Matrevi, F. Anto, N.B. Quashie, An improved SYBR Green-1-based fluorescence method for the routine monitoring of *Plasmodium falciparum* resistance to anti-malarial drugs, Malar. J. 14 (2015), https://doi.org/10.1186/s12936-015-1011-x 481.
[36] S. Sarkar, A.A. Siddiqui, S.J. Saha, R. De, S. Mazumder, C. Banerjee, M.S. Iqbal, S. Nag, S. Adhikari, U. Bandyopadhyay, Antimalarial activity of small-molecule benzothiazole hydrazones, Antimicrob. Agents Chemother. 60 (2016) 4217–4228, https://doi.org/10.1128/AAC.01575-15.
[37] S.J. Saha, A.A. Siddiqui, S. Pramanik, D. Saha, R. De, S. Mazumder, S. Debsharma, S. Nag, C. Banerjee, U. Bandyopadhyay, Hydrazonophenol, a food vacuole-targeted and ferriprotoporphyrin IX-interacting chemotype prevents drug-resistant malaria, ACS Infect Dis. 5 (2019) 63–73, https://doi.org/10.1021/acsinfecdis.8b00178.
[38] S. Sarkar, A.A. Siddiqui, S. Mazumder, R. De, S.J. Saha, C. Banerjee, Mohd.S. Iqbal, S. Adhikari, A. Alam, S. Roy, U. Bandyopadhyay, Ellagic acid, a dietary polyphenol, inhibits tautomerase activity of human macrophage migration inhibitory factor and its pro-inflammatory responses in human peripheral blood mononuclear cells, J. Agric. Food Chem. 63 (2015) 4988–4998, https://doi.org/10.1021/acs.jafc.5b00921.
[39] M.S. Iqbal, A.A. Siddiqui, C. Banerjee, S. Nag, S. Mazumder, R. De, S.J. Saha, S.K. Karri, U. Bandyopadhyay, Detection of retromer assembly in *Plasmodium falciparum* by immunosensing coupled to Surface Plasmon Resonance, Biochim. Biophys. Acta Proteins Proteomics 1866 (2018) 722–730, https://doi.org/10.1016/j.bbapap.2018.04.005.
[40] D.J. Sullivan, I.Y. Gluzman, D.G. Russell, D.E. Goldberg, On the molecular mechanism of chloroquine's antimalarial action, Proc. Natl. Acad. Sci. U. S. A. 93 (1996) 11865–11870, https://doi.org/10.1073/PNAS.93.21.11865.
[41] I.K. Srivastava, H. Rottenberg, A.B. Vaidya, Atovaquone, a broad spectrum antiparasitic drug, collapses mitochondrial membrane potential in a malarial parasite, J. Biol. Chem. 272 (1997) 3961–3966.
[42] X. Pan, S. Eathiraj, M. Munson, D.G. Lambright, TBC-domain GAPs for Rab GTPases accelerate GTP hydrolysis by a dual-finger mechanism, Nature 442 (2006) 303–306, https://doi.org/10.1038/nature04847.
[43] I. Simon, M. Zerial, R.S. Goody, Kinetics of interaction of Rab5 and Rab7 with nucleotides and magnesium ions, J. Biol. Chem. 271 (1996) 20470–20478, https://doi.org/10.1074/JBC.271.34.20470.
[44] J.O. Agola, L. Hong, Z. Surviladze, O. Ursu, A. Waller, J.J. Strouse, D.S. Simpson, C.E. Schroeder, T.I. Oprea, J.E. Golden, J. Aubé, T. Buranda, L.A. Sklar, A. Wandinger-Ness, A competitive nucleotide binding inhibitor: in vitro characterization of Rab7 GTPase inhibition, ACS Chem. Biol. 7 (2012) 1095–1108, https://doi.org/10.1021/cb3001099.
[45] N.S. Struck, S. Herrmann, C. Langer, A. Krueger, B.J. Foth, K. Engelberg, A.L. Cabrera, S. Haase, M. Treeck, M. Marti, A.F. Cowman, T. Spielmann, T.W. Gilberger, Plasmodium falciparum possesses two GRASP proteins that are differentially targeted to the Golgi complex via a higher- and lower-eukaryote-like mechanism, J. Cell Sci. 121 (2008) 2123–2129, https://doi.org/10.1242/jcs.021154.
[46] N.S. Struck, S. de Souza Dias, C. Langer, M. Marti, J.A. Pearce, A.F. Cowman, T.W. Gilberger, Re-defining the Golgi complex in *Plasmodium falciparum* using the novel Golgi marker PfGRASP, J. Cell Sci. 118 (2005) 5603–5613, https://doi.org/10.1242/jcs.02673.
[47] S. Hallée, J.A. Boddey, A.F. Cowman, D. Richard, Evidence that the *Plasmodium falciparum* protein sortilin potentially acts as an escorter for the trafficking of the rhoptry-associated membrane antigen to the rhoptries, MSphere 3 (2018), https://doi.org/10.1128/MSPHERE.00551-17 e00551–17.
[48] P.-J. Sloves, S. Delhaye, T. Mouveaux, E. Werkmeister, C. Slomianny, A. Hovasse, T. Dilezitoko Alayi, I. Callebaut, R.Y. Gaji, C. Schaeffer-Reiss, A. Van Dorsselear, V.B. Carruthers, S. Tomavo, Toxoplasma sortilin-like receptor regulates protein transport and is essential for apical secretory organelle biogenesis and host infection, Cell Host Microbe 11 (2012) 515–527, https://doi.org/10.1016/j.chom.2012.03.006.
[49] C. Aurrecoechea, J. Brestelli, B.P. Brunk, J. Dommer, S. Fischer, B. Gajria, X. Gao, A. Gingle, G. Grant, O.S. Harb, M. Heiges, F. Innamorato, J. Iodice, J.C. Kissinger, E. Kraemer, W. Li, J.A. Miller, V. Nayak, C. Pennington, D.F. Pinney, D.S. Roos, C. Ross, C.J. Stoeckert, C. Treatman, H. Wang, PlasmoDB: a functional genomic database for malaria parasites, Nucleic Acids Res. 37 (2009) D539–D543, https://doi.org/10.1093/nar/gkn814.
[50] F.B. Rached, C. Ndjembo-Ezougou, S. Chandran, H. Talabani, H. Yera, V. Dandavate, P. Bourdoncle, M. Meissner, U. Tatu, G. Langsley, Construction of a *Plasmodium falciparum* Rab-interactome identifies CK1 and PKA as Rab-effector kinases in malaria parasites, Biol. Cell. 104 (2012) 34–47, https://doi.org/10.1111/boc.201100081.
[51] F. Ben-Rached, G. Langley, Rab Proteins, Encyclopedia of Malaria, Springer, New York, New York, NY, 2013, pp. 1–11, https://doi.org/10.1007/978-1-4614-8757-9_36-1.
[52] M.N.J. Seaman, M.E. Harbour, D. Tattersall, E. Read, N. Bright, Membrane recruitment of the cargo-selective retromer subcomplex is catalysed by the small GTPase Rab7 and inhibited by the Rab-GAP TBC1D5, J. Cell Sci. 122 (2009) 2371–2382, https://doi.org/10.1242/jcs.048686.
[53] K.F. Suazo, C. Schaber, C.C. Palsuledesai, A.R. Odom John, M.D. Distefano, Global proteomic analysis of prenylated proteins in *Plasmodium falciparum* using an alkyne-modified isoprenoid analogue, Sci. Rep. 6 (2016), https://doi.org/10.1038/srep38615 38615.
[54] G. Modica, O. Skorobogata, E. Sauvageau, A. Vissa, C.M. Yip, P.K. Kim, H. Wurtele, S. Lefrancois, Rab7 palmitoylation is required for efficient endosome-to-TGN trafficking, J. Cell Sci. 130 (2017) 2579–2590, https://doi.org/10.1242/jcs.199729.
[55] M.L. Jones, M.O. Collins, D. Goulding, J.S. Choudhary, J.C. Rayner, Analysis of protein palmitoylation reveals a pervasive role in *Plasmodium* development and pathogenesis, Cell Host Microbe 12 (2012) 246–258, https://doi.org/10.1016/J.CHOM.2012.06.005.
[56] L.O. Sangaré, T.D. Alayi, B. Westermann, A. Hovasse, F. Sindikubwabo, I. Callebaut, E. Werkmeister, F. Lafont, C. Slomianny, M.-A. Hakimi, A. Van Dorsselaer, C. Schaeffer-Reiss, S. Tomavo, Unconventional endosome-like compartment and retromer complex in toxoplasma gondii govern parasite integrity and host infection, Nat. Commun. 7 (2016), https://doi.org/10.1038/ncomms11191 11191.
[57] M. Rug, A.G. Maier, Transfection of *Plasmodium falciparum*, Methods in Molecular Biology, 2012, pp. 75–98, , https://doi.org/10.1007/978-1-62703-026-7_6 Clifton, N.J..
[58] J.-H. Ch'Ng, K. Liew, A.S.-P. Goh, E. Sidhartha, K.S.-W. Tan, Drug-induced permeabilization of parasite's digestive vacuole is a key trigger of programmed cell

death in *Plasmodium falciparum*, Cell Death Dis. 2 (2011) e216, https://doi.org/10.1038/cddis.2011.97.
[59] H.C. Hoppe, D.A. van Schalkwyk, U.I.M. Wiehart, S.A. Meredith, J. Egan, B.W. Weber, Antimalarial quinolines and artemisinin inhibit endocytosis in *Plasmodium falciparum*, Antimicrob. Agents Chemother. 48 (2004) 2370–2378, https://doi.org/10.1128/AAC.48.7.2370-2378.2004.
[60] A.M. Tomlins, F. Ben-Rached, R.A. Williams, W.R. Proto, I. Coppens, U. Ruch, T.W. Gilberger, G.H. Coombs, J.C. Mottram, S. Müller, G. Langsley, *Plasmodium falciparum* ATG8 implicated in both autophagy and apicoplast formation, Autophagy 9 (2013) 1540–1552, https://doi.org/10.4161/auto.25832.
[61] M.R. Spinosa, C. Progida, A. De Luca, A.M.R. Colucci, P. Alifano, C. Bucci, Functional characterization of Rab7 mutant proteins associated with Charcot-Marie-Tooth type 2B disease, J. Neurosci. 28 (2008) 1640–1648, https://doi.org/10.1523/JNEUROSCI.3677-07.2008.
[62] Y. Lin, C. Wu, X. Wang, T. Kemper, A. Squire, M. Gunzer, J. Zhang, X. Chen, M. Lu, Hepatitis B virus is degraded by autophagosome-lysosome fusion mediated by Rab7 and related components, Protein Cell 10 (2019) 60–66, https://doi.org/10.1007/s13238-018-0555-2.
[63] C.N. Ezougou, F. Ben-Rached, D.K. Moss, J. Lin, S. Black, E. Knuepfer, J.L. Green, S.M. Khan, A. Mukhopadhyay, C.J. Janse, I. Coppens, H. Yera, A.A. Holder, G. Langsley, *Plasmodium falciparum* Rab5B is an N-terminally MYRISTOYLATED Rab GTPase that is targeted to the parasite's plasma and food vacuole membranes, PLoS One 9 (2014), https://doi.org/10.1371/journal.pone.0087695 e87695.
[64] M. Lamarque, C. Tastet, J. Poncet, E. Demettre, P. Jouin, H. Vial, J.-F. Dubremetz, Food vacuole proteome of the malarial parasite *Plasmodium falciparum*, Proteomics Clin. Appl. 2 (2008) 1361–1374, https://doi.org/10.1002/prca.200700112.
[65] C. Bucci, P. Thomsen, P. Nicoziani, J. McCarthy, B. van Deurs, Rab7: a key to lysosome biogenesis, Mol. Biol. Cell 11 (2000) 467–480, https://doi.org/10.1091/mbc.11.2.467.